Martínez-Bisbal, M.; Martínez-Granados, B.; Rovira, V.; Celda, B.; Esteve, V. (2015). Magnetic resonance spectroscopy and imaging on fresh human brain tumor biopsies at microscopic resolution. Analytical and Bioanalytical Chemistry. 407(22):6771-6780. doi:10.1007/s00216-015-8847-3.

Magnetic resonance spectroscopy and imaging on fresh human brain tumour biopsies at microscopic resolution.

M. Carmen Martínez-Bisbal[a,b], Beatriz Martínez-Granados[a,c], Vicente Rovira[d], Bernardo Celda[a], Vicent Esteve[a,c]

a. Department of Physical Chemistry, University of Valencia, Valencia, Spain
b. Centre for Molecular Recognition and Technologic Development (IDM), Polytechnic University of Valencia, Valencia, Spain
c. Networking Research Center on Bioengineering, Biomaterials and Nanomedicine (CIBER-BBN), Valencia, Spain
d. Neurosurgery Service, Hospital La Ribera, Alzira, Spain

Corresponding author:
Vicent Esteve
e-mail: vicent.esteve@uv.es
Full address: Department of Physical Chemistry, University of Valencia
C/ Dr. Moliner 50, 46100 Burjassot, Valencia SPAIN
Telephone/Fax: 0034963543213

Abbreviations

MR: magnetic resonance; MRI: magnetic resonance imaging; MRS: magnetic resonance spectroscopy; HR-MAS: high resolution magic angle spinning spectroscopy; MRM: magnetic resonance microscopy; GBM: glioblastoma multiform; FLASH: fast low angle shot; RARE: rapid acquisition with relaxation enhancement; PRESS: point resolved spectroscopy; H&E: hematoxylin and eosin; VAPOR: Variable pulse power and optimized relaxation delays; NAA: N-Acetylaspartate; PFA: para-formaldehyde; PBS: phosphate buffered saline, OM: optical microscopy

Abstract

The metabolic composition and concentration knowledge provided by MRS liquid and HR-MAS has a relevant impact in the clinical practice during MRI monitoring of human tumours. In addition, the combination of morphological and chemical information by MRI and MRS has been particularly useful for diagnosis and prognosis of their evolution. MRI spatial resolution reachable in human beings is limited for safety reasons and the demanding necessary conditions are only applicable on experimental model animals. Nevertheless, MRS and MRI can be done on human biopsies at high spatial resolution, enough to allow a direct correlation between the chemical information and the histological features observed in such biopsies.

Although HR-MAS is nowadays a well established technique for spectroscopic analysis of tumour biopsies, with this approach just a mean metabolic profile of the whole sample can be obtained and thus the high histological heterogeneity of some important tumours is mostly neglected. The value of metabolic HR-MAS data strongly depends in a wide statistical analysis and usually the microanatomical rationale for the correlation between histology and spectroscopy is lost.

We present here a different approach for the combined use of MRI and MRS on fresh human brain tumour biopsies with native contrast. This approach has been designed to achieve high spatial (18x18x50 µm) and spectral (0.031 µl) resolution in order to obtain as much as possible spatially detailed morphological and metabolical information without any previous treatment that can alter the sample. The preservation of native tissue conditions can provide information that can be translated to in vivo studies and additionally opens the possibility of performing other techniques to obtain complementary information from the same sample.

Keywords:

Magnetic Resonance Imaging, Magnetic Resonance Spectroscopy, Magnetic Resonance Microscopy, HR-MAS: High Resolution Magic Angle Spinning Spectroscopy , biopsy, human brain tumour, fresh tissue, glioblastoma

Introduction

The clinical application of MRI and MRS for in vivo study has provided a non-invasive way for a detailed analysis of the morphology and biochemistry of human brain tumours [1-6]. MRI and MRS have yield valuable information in important clinical questions as the discrimination between neoplastic and non neoplastic lesions [7-11], the human brain tumour type identification and grade determination [1-3, 12-17], the discrimination between primary tumour and metastases [18], and the detection of tumour infiltration to the normal appearing tissue and to the edema region [12, 19, 20]. Moreover, MRS combined with MRI has also been useful in the follow up of treated lesions, distinguishing between necrosis and tumour progression [21, 22] and has given biochemical information to delineate the tumour extent to refine the radiotherapy target and the surgical treatment [23, 24]. However, the in vivo morphological and biochemical information that can be obtained in patients is limited by the low magnetic fields used in the clinical settings (usually 1.5-3T).

MRM (sometimes defined as high resolution MRI acquired with a resolution less than 100 µm in at least one dimension [25]) is an imaging method that has become in a valuable technique for translational and preclinical studies of human neurological diseases [26]. The ex vivo study of biological tissues and organs by MRM allows higher spatial resolution and longer times of study without motion artifacts [27] and, thus can provide morphological details that would be very difficult or almost impossible to be achieved on in vivo studies. In human tissue samples, the ex vivo study of cerebral cortex [28] and hippocampus [29] pieces at 9.4 T and visual cortex [30] at 14 T, has provided cytoarchitectonic details on the different structures with a resolution of 78x78x500, 200x200x200 and 80x80x80 µm respectively.

Nevertheless, the examples of ex vivo imaging studies of human brain tumour tissues by MRI microscopy are scarce. Excised tissue of human cerebral cavernous malformations has been studied by MRI microscopy at 9.4 and 14 T with isotropic resolution of 60 μm allowing the study of the angioarchitecture of these lesions near the histological resolution [31]. Diverse type of meningeoma and glioma human brain tumour samples have been studied by MRI microscopy at 14T with resolution of 34x34x500 μm allowing the observation of fine tissue features [32]. All the human tissue samples included in these ex vivo MRM studies were formalin-fixed samples [28-32] and in some cases the tissues were also treated with novel strategies for target-specific contrast agents [30]. In addition, the fixative processes in biopsy and autopsy tissue studies have been demonstrated to alter the tissue properties [27, 33, 34]. The use of fixative substances can dramatically modify the concentration of the metabolites, contaminate the sample and change the relaxation times of the tissue. This prevents the biochemical study of these samples by MRS and thus, molecular MRI cannot be obtained and then be superimposed with the high resolution MRI images as it can be done with lower resolution in vivo in patients [1, 5, 9, 10, 19, 23, 24].

A combination of MRS and MRM has been successfully applied in vivo to study the brain metabolites in rats [35-37]. The use of a very short echo time (1 ms), FASTMAP shimming performance [38] and VAPOR water suppression has yielded a highly resolved in vivo ^{1}H MRS spectra in rat brain where resonances from alanine, aspartate, choline group, creatine, GABA, glucose, glutamate, glutamine, myo-Inositol, lactate, N-acetylaspartate, N-acetylaspartylglutamate, phosphocreatine, glycogen and taurine have been detected [35]. The tissue concentrations of these metabolites and others as phosphorylethanolamine and scyllo-inositol, have been quantified in the rat brain showing a good agreement with the neurochemical data from the literature [36]. The selection of the right echo time has enabled to target especially some signals as glucose to estimate in vivo concentrations as an alternative to observe the uptake detected by nuclear medicine [39]. A comprehensive evaluation of cerebral energy metabolism in rat brain using infusions of [1-^{13}C] D-glucose with simultaneous measurement of lactate, glucose and phosphocreatine has been feasible with the use of sequences to select the signals of ^{1}H bound to ^{13}C [37]. Other metabolites as glutamate, glutamine and GABA have been also shown to incorporate ^{13}C [37].

The brain tumours studied by MRI and MRS microscopy are usually gliomas, intracranial neoplasms that are originated from neuroglial cells, and that are the most common of the primary brain tumours [52]. Glioblastoma multiform (GBM) is the highest glioma grade type and the most common malignant tumour currently found in the central nervous system in adults [53]. MRI studies in human GBM reveal these tumours as a poorly delineated mass with areas of necrosis, cyst formation and edema [52]. Microscopically, the salient features are the diversity of cell forms, the dense cellularity, the presence of focal necrosis and the vascular changes both inside and adjacent to the tumour [52]. Microvascular proliferation is present in 95% of GBM and provides the basis for malignancy grading of glioma tumours [52, 54]. The identification of the border zone between tumour infiltrated and normal brain tissue is one of the major problems to be solved before starting the therapy. These invasive regions of tumour are often missed by routine MRI techniques and are usually the reason for tumour regrowth or recurrence after surgery and radiotherapy [23].

In this study, MRI and MRS microscopy are combined to evaluate the possibility of obtaining spatially localized biochemical information together with 3D vascular and cytoarchitectural features on human GBM biopsies. Previously published work supports the possibility of a metabolic study by MRS in intact human brain biopsies with single voxel and low resolution MRI images [55]. In this work, the MRI signal to noise has been significantly improved and then the MRI resolution obtained is enough to allow a direct comparison between microanatomical details and the histological analysis used here as reference. Moreover, multivoxel spectra provide a spatially distributed metabolic information, complementary to the single voxel, as it can be seen in the study of tumours in animals by MRS and MRM [40-51]. This detailed metabolic and structural information could be of main importance in the prognosis of GBM tumours. This study has been performed using native contrast and the sample has not been modified by fixative process in order to make possible the MRS study and open the possibility for further additional ex vivo studies on the same samples as DNA chips, proteomics, immunohistochemistry, or imaging mass spectrometry. These techniques could provide valuable additional biochemical information for improving classification, prognosis and treatment selection on brain tumours.

Materials and methods

This study was approved by the Ethics Committee of the Hospital de la Ribera. The biopsies used in this study come from patients that underwent surgical resection of brain tumour. A portion of the tissue biopsy was stored at -80ºC until the NMR microscopy study was performed. Other portion underwent routine histological analyses for clinical diagnosis. The tumours were identified as GBM (see table 1).

The samples were studied by MRS and MRI in a 14 T magnet (Avance DRX 600 spectrometer, Bruker, Rheinstetten, Germany) operating at 600.13 MHz for ^{1}H and connected to a microimage console with a gradient system of 300 G/cm at 60 A current (Bruker Biospin). The instrument was equipped with a standard bore Micro 5 imaging probehead with rf inserts of 5 (for samples 1-5 and 8) and 10 mm (for samples 6 and 7). A Bruker Cooling Unit Extreme controlled the temperature during the acquisition.

Human brain biopsy handling and sample preparation

Each sample was studied fresh, without any other treatment than the ultrafreezing after the surgical process. No fixative process or enhancing contrast agent was added to the samples. The samples were introduced in NMR tubes of 5 or 10 mm, according to the tissue sample size. Inside the tubes, the samples were submerged in cool PBS to avoid saline stress of the tissue and to get high amount of proton signal to prepare and perform the MRI and MRS study. The probe was precooled before introducing the samples to minimize the effects of tissue degradation. The acquisition was carried out at a theoretical temperature of 3ºC. This value corresponds to the temperature measured from the thermocouple, but internal measurement using a 100% methanol sample provided a corrected internal value of 4ºC.

MRI experiments

Orthogonal FLASH (Fast Low Angle Shot) images were acquired for the initial sample location inside the tube and inspection of the sample position inside the probe (field of view

10x10 mm, matrix size 128x128 elements, slice thickness 1 mm, TR/TE 100/5 ms, 4 averages, 51 seconds).

Multislice RARE (Rapid Acquisition with Relaxation Enhancement) images in the three planes were acquired in a short acquisition time (13 minutes) to achieve better detail before planning the high resolution images (field of view 4.5x4.5 – 6.5x6.5 mm, matrix 256x256, TR/TE_f 4200/36 ms, RARE factor 8, 8 averages, 13 minutes). These rapid RARE images had 500 μm of thickness and the in plane spatial resolution was 16x16 μm.

Multislice RARE sequence was also used for obtaining the highest resolution images with slice thickness of 50 μm (field of view 4.5x4.5 – 6.5x6.5 mm, matrix 256x256, TR/TE_f 4630/36 ms, RARE factor 8, 128 averages). The MRI spatial resolution achieved was 16x16x50 μm.

MRS experiments

Single voxel (SV) and multivoxel (MV) experiments were acquired for all tumour biopsies with PRESS (Point RESolved Spectroscopy) sequence.

A MV slice was located in the tissue, in parallel to the high resolution RARE images, including the tissue and the surrounding solution. The slice thickness was 500 μm. The resolution was of 250x250x500 μm (0.031 μL of volume). FASTMAP procedure (1^{st} and 2^{nd} order automatic shim algorithm [38]) was used for field homogenization performance. The water suppression was achieved by VAPOR pulse sequence [35] (Variable pulse power and optimized relaxation delays). TE was 12 ms and TR 2100 ms and with 2k points in time domain.

SV (size ranging from 1x1x1 mm, 1μL, to 2x2x2 mm, 8μL, TR/TE 2100/12 ms) were located in the tissue for each biopsy. In order to optimize the 1^{st} order shims a specific shimming was performed on the selected volume for each single voxel before the acquisition. VAPOR sequence was used for water suppression. The spectral width was 10 ppm/6000 Hz and the number of points was 4k.

Histological study

The samples underwent routine histological procedures after the MR microscopy study. The samples were immersed in 10% formalin inside the NMR tubes. Once fixed, the tissue specimens were embedded in paraffin, and the tissue pieces were serially sectioned into 5 µm slices and H&E stained.

Results and discussion

The ex vivo NMR microscopy study on fresh biopsies of human GBM was performed trying to cause minimum alterations on the sample. With this objective the sample was submerged in PBS and kept at low temperature during the experiments. Using RARE pulse sequence 'thick' (500 µm) and 'thin' (50µm) slices were obtained with an in plane resolution of 16x16 µm. RARE images with 500 µm of thickness made possible a rapid identification of the sample location (Figure 1A) as well as the detection of some regional differences, as blood vessels, that could be observed throughout the tissue, even at this moderate resolution. RARE images at 50 µm of thickness (Figure 1B and C) showed a higher level of detail in the tissue in all the samples compared to the images at 500 µm of thickness. This improvement in the resolution was enough to clearly show the microheterogeneity that could be afterwards appreciated in the histological preparation (Figure 1 D). Moreover, the improved sharpness permitted the observation of fine micronanatomical details in the structure of the tissues, as it can be appreciated in the fibber-like texture present in some parts of the tissue (Figure 1, B and C). The changes in the tissue contrast by MRI were also observed in the differently stained parts of the H&E slices corresponding to the diverse types of tissue that constituted the sample (Figure 1D). The MRS experiments provided the metabolite profile corresponding to each part of the sample and the resonances of small metabolites as Lactate, Creatine, Choline, Glutamine, Glutamate, N-Acetylaspartate and Alanine among others were easily detected (Figure 1E). On this sample, three types of tissues with clear differences in contrast could be distinguished. On the lower and left part the grey areas in MRI appear poorly stained in optical microscopy (OM) and could be related to a most necrotic area (Figure 1E, boxes 5 and 6). On the middle-right part a white and bright area in MRI that is more intensely stained

by H&E could be related to a more viable tissue (Figure 1E, boxes 3 and 4). In the upper part of the sample the MRI images show a very dark area which, as seen in OM, contains a high amount of red blood cells that can be related to a hemorrhagic area (Figure 1E, boxes 1 and 2). These dark areas on T2 weighted MRI images are normally associated with the presence of deoxyhemoglobin or hemosiderin. The mean spectrum for this sample can be seen at the bottom of the figure 1E and it is the result of the contribution of very different types of tissue (and metabolic composition). These spectra can be compared with the ones obtained on a different piece of the same biopsy (Figure 1F). This whole volume spectrum is similar to the mean spectra displayed in figure 1E, but whit this information alone we cannot say if the differences (for example the different proportions of Gln and Glu) are due to distinct metabolic profiles in the tissue or simply a different proportion of the same profiles.

In some samples, despite the fact that hyperplasia and tortuous vasculature was observed (Figure 2, A and B), the tissue is rather homogenous and the spectra in different areas are very similar (Figure 2C). Nevertheless, still some minor differences could be present (Figure 2D). The signals of Lactate, Alanine, Glutamate, Creatine, Choline and aminoacids can be observed in the three chosen locations with slight differences in the intensity. In this case, the mean spectra of the sample will be representative because the entire sample seems to be mostly constituted by a specific type of tissue.

Noteworthy, a very necrotic sample can still display heterogeneous contrast and texture (Figure 3, A and B). The sample of this tumour was mainly composed of lipids, as shown in the spectra in the figure 3C. The different hydrogen peaks from several saturated and unsaturated carbons in the fatty acid are assigned in a spectrum taken from the multivoxel experiment (figure 3C) and a density map showing their distribution has been constructed using the intensity of–CH=CH– hydrogen resonances at 5.34 ppm (figure 3C, left). Differences in the proportions of the signals can be observed in each one of the selected locations, which is indicative of a heterogeneous lipidic composition. These heterogeneities in the structure and composition of the residual necrotic lipids could be due to different kinds of original constituting tissues.

HR-MAS is other NMR technique widely used to obtain high resolution spectra on tissue samples [56-61]. Despite the speed and resolution that this technique can provide, the biochemical interpretation of HR-MAS spectra is limited owing, on the one hand, to the fact that the spectra obtained are the mean contribution from all the sample introduced in the rotor, and on the other hand the high spinning speed needed in HR-MAS originates great distortion of the tissue and transference of metabolites from the tissue to the medium [55]. With the use of MRS microscopy the knowledge of spatial distribution of the metabolites is available and the contribution of different type of tissue within the sample can be evaluated. Moreover, in MRS microscopy the size of the sample may be larger than in HR-MAS studies and without the distortions due to the spinning. These advantages of MRS microscopy over HR-MAS are especially important for the study of intrinsically heterogeneous tissues as is the case on some tumours like GBM.

The application of MRI and MRS to the study of metabolism of tumours in vivo in animal models has provided a high metabolical detail [39-51]. Some of the research has aimed for the study of tumour metabolism in general [41, 47-48] with different objectives as to distinguish between two distinct glioblastoma phenotypes [41] or different glioma models [47] and to detect the intense glycolysis in the tumour cells [48]. Other part of the research in tumours has demonstrated the value of these techniques to evidence the distribution of a determined metabolite or group of metabolites as lactate, choline, creatine and N-acetylaspartate (NAA) [46, 49] and unsaturated mobile lipids [42-45, 50-51]. NAA was essentially present in the normal tissue outside the tumor, choline was higher near the periphery, creatine was low near the center of the tumour and lactate was detected almost exclusively within the tumors [46, 49]. The unsaturated mobile lipids were related with treatment-induced apoptosis [42-45, 50] and the saturated mobile lipids were found in areas with necrosis [51]. In this context, MRS has also been useful to verify the value of this technique to study the tumour pH in the tumour microenvironment using probe molecules [46, 49] and has shown acidic pH in the nonviable part of tumours and normal pH in the viable tumour areas [49]. MRS has also been used from a metabonomic perspective studying the perturbation of in vivo metabolism with acute hyperglycemia in mice brain tumours observing maximal increases in glucose resonances in tumors compared to control mice

group, which is in agreement with extracellular accumulation of glucose and with glucose transport/metabolism working close to the maximum capacity in these tumours [40]. The extracellular pH in gliomas has been shown also altered after glucose infusion [46]. These experiments have been usually performed at short echo times in order to achieve as much as possible metabolical information. Since T2 effects are minimized, more molecules can be detected and the identification of coupled spin systems is improved [35, 36]. In some of these studies single voxel (volumes of 27-125 μL) experiments have been performed to obtain the metabolical profile of the tumour and the contralateral location [40-41, 44], while in the other studies, multivoxel sequences have provided a detailed spatial distribution of the metabolites [42-43, 46] with volumes ranging from 0.75 to 5 μL per voxel.Aside of the spectrospopic analysis, we have checked that NMR microscopy o MRM) allows a three-dimensional microanatomical study of these samples. We have performed the analysis of the vasculature on a human GBM biopsy obtaining a 3D model of the vessels distribution and ramifications inside the whole sample (Figure 4). Additionally, virtual sections can be done in any desired orientation in order to carry precise measurements of the vessels diameter and points of ramification (Figure 4C,D). The spatial resolution in this study is out of reach of the clinical application of MRI. The images at 500 μm of thickness have also shown differences in contrast inside the samples and have presented some details that, despite of being better interpreted with the higher resolution sections, themselves can provide a kind of intermediate step between high resolution MRM or OM and the in vivo human MRI studies. Regarding the MRS sequences, the small volumes measured in multivoxel (0.031μL) and single voxel (1μL) experiments have provided spatially localized information on the metabolite and the lipids present in these kind of tumours. In this study the GBM biopsy samples were very different according to the MRI, MRS and histological findings, in terms of metabolite content, image contrast and vascularisation. The pixel resolution in MRI has enabled to observe small blood vessels, regions with several textures and areas with different natural contrast in agreement with the subsequent histological study.

Conclusions

This study shows the feasibility for performing NMR microscopy on fresh human brain biopsies in PBS without fixation or other treatments. The high resolution images and spectra here obtained have provided localized metabolic information and a morphological analysis at microscale level. The multimodal data obtained from the three techniques (MRI, MRS and OM) offers complementary and concurrent information on the tissue features key for the human brain tumours study.

The approach here proposed can complement other techniques like HR-MAS in the rationalization of the results and interpreting the variable contribution of several kinds of tissue that can be present in different proportions in each sample.

The performance of this study on human tumour tissue permits a more direct comparison with animal models studied in vivo and ex vivo also at high resolution. Moreover, it can help to knowledge transfer from high resolution MRI and MRS microscopy data to MRI and MRS in the clinical practice.

Acknowledgements

The authors acknowledge the SCSIE-University of Valencia Microscopy Service for the histological preparations. They also acknowledge financial support from the Spanish Government project SAF2007-6547, the Generalitat Valenciana project GVACOMP2009-303, and the E.U.'s VI Framework Programme via the project "Web accessible MR decision support system for brain tumour diagnosis and prognosis, incorporating in vivo and ex vivo genomic and metabolomic data" (FP6-2002-LSH 503094)..

References

1. Stadlbauer A, Gruber S, Nimsky C, Fahlbusch R, Hammen T, Buslei R, Tomandl B, Moser E, Ganslandt O (2006) Preoperative grading of gliomas by using metabolite quantification with high-spatial-resolution proton MR spectroscopic imaging. Radiology 238:958

2. Howe FA, Barton SJ, Cudlip SA, Stubbs M, Saunders DE, Murphy M, Wilkins P, Opstad KS, Doyle VL, McLean MA, Bell BA, Griffiths JR (2003) Metabolic profiles of human brain tumors using quantitative in vivo 1H magnetic resonance spectroscopy. Magn Reson Med 49:223

3. Castillo M, Kwock L (1999) Clinical applications of proton magnetic resonance spectroscopy in the evaluation of common intracranial tumors. Top Magn Reson Imaging 10:104

4. Howe FA, Opstad KS (2003) 1H MR spectroscopy of brain tumours and masses. NMR Biomed 16:123

5. Martinez-Bisbal MC, Celda B (2009) Proton magnetic resonance spectroscopy imaging in the study of human brain cancer. Q J Nucl Med Mol Imaging 53:618

6. Sibtain NA, Howe FA, Saunders DE (2007) The clinical value of proton magnetic resonance spectroscopy in adult brain tumours. Clin Radiol 62:109

7. Tong Z, Yamaki T, Harada K, Houkin K (2004) In vivo quantification of the metabolites in normal brain and brain tumors by proton MR spectroscopy using water as an internal standard. Magn Reson Imaging 22:1017

8. Hourani R, Brant LJ, Rizk T, Weingart JD, Barker PB, Horska A (2008) Can proton MR spectroscopic and perfusion imaging differentiate between neoplastic and nonneoplastic brain lesions in adults? AJNR Am J Neuroradiol 29:366

9. Hourani R, Horska A, Albayram S, Brant LJ, Melhem E, Cohen KJ, Burger PC, Weingart JD, Carson B, Wharam MD, Barker PB (2006) Proton magnetic resonance spectroscopic imaging to differentiate between nonneoplastic lesions and brain tumors in children. J Magn Reson Imaging 23:99

10. Lai PH, Weng HH, Chen CY, Hsu SS, Ding S, Ko CW, Fu JH, Liang HL, Chen KH (2008) In vivo differentiation of aerobic brain abscesses and necrotic glioblastomas multiforme using proton MR spectroscopic imaging. AJNR Am J Neuroradiol 29:1511

11. Vuori K, Kankaanranta L, Hakkinen AM, Gaily E, Valanne L, Granstrom ML, Joensuu H, Blomstedt G, Paetau A, Lundbom N (2004) Low-grade gliomas and focal cortical developmental malformations: differentiation with proton MR spectroscopy. Radiology 230:703

12. Di Costanzo A, Scarabino T, Trojsi F, Popolizio T, Catapano D, Giannatempo GM, Bonavita S, Portaluri M, Tosetti M, d'Angelo VA, Salvolini U, Tedeschi G (2008)

Proton MR spectroscopy of cerebral gliomas at 3 T: spatial heterogeneity, and tumour grade and extent. Eur Radiol 18:1727

13. Law M, Yang S, Wang H, Babb JS, Johnson G, Cha S, Knopp EA, Zagzag D (2003) Glioma grading: sensitivity, specificity, and predictive values of perfusion MR imaging and proton MR spectroscopic imaging compared with conventional MR imaging. AJNR Am J Neuroradiol 24:1989

14. Catalaa I, Henry R, Dillon WP, Graves EE, McKnight TR, Lu Y, Vigneron DB, Nelson SJ (2006) Perfusion, diffusion and spectroscopy values in newly diagnosed cerebral gliomas. NMR Biomed 19:463

15. Devos A, Lukas L, Suykens JA, Vanhamme L, Tate AR, Howe FA, Majos C, Moreno-Torres A, van der Graaf M, Arus C, Van Huffel S (2004) Classification of brain tumours using short echo time 1H MR spectra. J Magn Reson 170:164

16. Burtscher IM, Skagerberg G, Geijer B, Englund E, Stahlberg F, Holtas S (2000) Proton MR spectroscopy and preoperative diagnostic accuracy: an evaluation of intracranial mass lesions characterized by stereotactic biopsy findings. AJNR Am J Neuroradiol 21:84

17. Ishimaru H, Morikawa M, Iwanaga S, Kaminogo M, Ochi M, Hayashi K (2001) Differentiation between high-grade glioma and metastatic brain tumor using single-voxel proton MR spectroscopy. Eur Radiol 11:1784

18. Sjobakk TE, Johansen R, Bathen TF, Sonnewald U, Kvistad KA, Lundgren S, Gribbestad IS (2007) Metabolic profiling of human brain metastases using in vivo proton MR spectroscopy at 3T. BMC Cancer 7:141

19. Stadlbauer A, Nimsky C, Buslei R, Pinker K, Gruber S, Hammen T, Buchfelder M, Ganslandt O (2007) Proton magnetic resonance spectroscopic imaging in the border zone of gliomas: correlation of metabolic and histological changes at low tumor infiltration--initial results. Invest Radiol 42:218

20. Law M, Cha S, Knopp EA, Johnson G, Arnett J, Litt AW (2002) High-grade gliomas and solitary metastases: differentiation by using perfusion and proton spectroscopic MR imaging. Radiology 222:715

21. Schlemmer HP, Bachert P, Herfarth KK, Zuna I, Debus J, van Kaick G (2001) Proton MR spectroscopic evaluation of suspicious brain lesions after stereotactic radiotherapy. AJNR Am J Neuroradiol 22:1316

22. Weybright P, Sundgren PC, Maly P, Hassan DG, Nan B, Rohrer S, Junck L (2005) Differentiation between brain tumor recurrence and radiation injury using MR spectroscopy. AJR Am J Roentgenol 185:1471

23. Stadlbauer A, Moser E, Gruber S, Buslei R, Nimsky C, Fahlbusch R, Ganslandt O (2004) Improved delineation of brain tumors: an automated method for segmentation based on pathologic changes of 1H-MRSI metabolites in gliomas. Neuroimage 23:454

24. Dowling C, Bollen AW, Noworolski SM, McDermott MW, Barbaro NM, Day MR, Henry RG, Chang SM, Dillon WP, Nelson SJ, Vigneron DB (2001) Preoperative proton MR spectroscopic imaging of brain tumors: correlation with histopathologic analysis of resection specimens. AJNR Am J Neuroradiol 22:604

25. Benveniste H, Blackband S (2002) MR microscopy and high resolution small animal MRI: applications in neuroscience research. Prog Neurobiol 67:393

26. Benveniste H, Blackband SJ (2006) Translational neuroscience and magnetic-resonance microscopy. Lancet Neurol 5:536

27. Thelwall PE, Shepherd TM, Stanisz GJ, Blackband SJ (2006) Effects of temperature and aldehyde fixation on tissue water diffusion properties, studied in an erythrocyte ghost tissue model. Magn Reson Med 56:282

28. Fatterpekar GM, Naidich TP, Delman BN, Aguinaldo JG, Gultekin SH, Sherwood CC, Hof PR, Drayer BP, Fayad ZA (2002) Cytoarchitecture of the human cerebral cortex: MR microscopy of excised specimens at 9.4 Tesla. AJNR Am J Neuroradiol 23:1313

29. Yushkevich PA, Avants BB, Pluta J, Das S, Minkoff D, Mechanic-Hamilton D, Glynn S, Pickup S, Liu W, Gee JC, Grossman M, Detre JA (2009) A high-resolution computational atlas of the human hippocampus from postmortem magnetic resonance imaging at 9.4 T. Neuroimage 44:385

30. Blackwell ML, Farrar CT, Fischl B, Rosen BR (2009) Target-specific contrast agents for magnetic resonance microscopy. Neuroimage 46:382

31. Shenkar R, Venkatasubramanian PN, Zhao JC, Batjer HH, Wyrwicz AM, Awad IA (2008) Advanced magnetic resonance imaging of cerebral cavernous malformations: part I. High-field imaging of excised human lesions. Neurosurgery 63:782

32. Gonzalez-Segura A, Morales JM, Gonzalez-Darder JM, Cardona-Marsal R, Lopez-Gines C, Cerda-Nicolas M, Monleon D (2011) Magnetic resonance microscopy

at 14 Tesla and correlative histopathology of human brain tumor tissue. PLoS One 6:e27442

33. Shepherd TM, Flint JJ, Thelwall PE, Stanisz GJ, Mareci TH, Yachnis AT, Blackband SJ (2009) Postmortem interval alters the water relaxation and diffusion properties of rat nervous tissue — Implications for MRI studies of human autopsy samples. Neuroimage 44:820

34. Grinberg LT, Amaro E,Jr, Teipel S, dos Santos DD, Pasqualucci CA, Leite RE, Camargo CR, Goncalves JA, Sanches AG, Santana M, Ferretti RE, Jacob-Filho W, Nitrini R, Heinsen H, Brazilian Aging Brain Study Group (2008) Assessment of factors that confound MRI and neuropathological correlation of human postmortem brain tissue. Cell Tissue Bank 9:195

35. Tkac I, Starcuk Z, Choi IY, Gruetter R (1999) In vivo 1H NMR spectroscopy of rat brain at 1 ms echo time. Magn Reson Med 41:649

36. Pfeuffer J, Tkac I, Provencher SW, Gruetter R (1999) Toward an in vivo neurochemical profile: quantification of 18 metabolites in short-echo-time (1)H NMR spectra of the rat brain. J Magn Reson 141:104

37. Pfeuffer J, Tkac I, Choi IY, Merkle H, Ugurbil K, Garwood M, Gruetter R (1999) Localized in vivo 1H NMR detection of neurotransmitter labeling in rat brain during infusion of [1-13C] D-glucose. Magn Reson Med 41:1077

38. Gruetter R (1993) Automatic, localized in vivo adjustment of all first- and second-order shim coils. Magn Reson Med 29:804

39. Steinberg JD, Velan SS (2012) Measuring glucose concentrations in the rat brain using echo-time-averaged point resolved spectroscopy at 7 tesla. Magnetic Resonance in Medicine:n/a

40. Simoes RV, Garcia-Martin ML, Cerdan S, Arus C (2008) Perturbation of mouse glioma MRS pattern by induced acute hyperglycemia. NMR Biomed 21:251

41. Thorsen F, Jirak D, Wang J, Sykova E, Bjerkvig R, Enger PO, van der Kogel A, Hajek M (2008) Two distinct tumor phenotypes isolated from glioblastomas show different MRS characteristics. NMR Biomed 21:830

42. Liimatainen T, Hakumaki J, Tkac I, Grohn O (2006) Ultra-short echo time spectroscopic imaging in rats: implications for monitoring lipids in glioma gene therapy. NMR Biomed 19:554

43. Liimatainen TJ, Erkkila AT, Valonen P, Vidgren H, Lakso M, Wong G, Grohn OH, Yla-Herttuala S, Hakumaki JM (2008) 1H MR spectroscopic imaging of phospholipase-mediated membrane lipid release in apoptotic rat glioma in vivo. Magn Reson Med 59:1232

44. Liimatainen T, Hakumaki JM, Kauppinen RA, Ala-Korpela M (2009) Monitoring of gliomas in vivo by diffusion MRI and (1)H MRS during gene therapy-induced apoptosis: interrelationships between water diffusion and mobile lipids. NMR Biomed 22:272

45. Griffin JL, Lehtimaki KK, Valonen PK, Grohn OH, Kettunen MI, Yla-Herttuala S, Pitkanen A, Nicholson JK, Kauppinen RA (2003) Assignment of 1H nuclear magnetic resonance visible polyunsaturated fatty acids in BT4C gliomas undergoing ganciclovir-thymidine kinase gene therapy-induced programmed cell death. Cancer Res 63:3195

46. Provent P, Benito M, Hiba B, Farion R, Lopez-Larrubia P, Ballesteros P, Remy C, Segebarth C, Cerdan S, Coles JA, Garcia-Martin ML (2007) Serial in vivo spectroscopic nuclear magnetic resonance imaging of lactate and extracellular pH in rat gliomas shows redistribution of protons away from sites of glycolysis. Cancer Res 67:7638

47. Doblas S, He T, Saunders D, Hoyle J, Smith N, Pye Q, Lerner M, Jensen RL, Towner RA (2012) In vivo characterization of several rodent glioma models by 1H MRS. NMR Biomed 25:685

48. Ziegler A, von Kienlin M, Decorps M, Remy C (2001) High glycolytic activity in rat glioma demonstrated in vivo by correlation peak 1H magnetic resonance imaging. Cancer Res 61:5595

49. Garcia-Martin ML, Herigault G, Remy C, Farion R, Ballesteros P, Coles JA, Cerdan S, Ziegler A (2001) Mapping extracellular pH in rat brain gliomas in vivo by 1H magnetic resonance spectroscopic imaging: comparison with maps of metabolites. Cancer Res 61:6524

50. Hakumaki JM, Poptani H, Sandmair AM, Yla-Herttuala S, Kauppinen RA (1999) 1H MRS detects polyunsaturated fatty acid accumulation during gene therapy of glioma: implications for the in vivo detection of apoptosis. Nat Med 5:1323

51. Zoula S, Herigault G, Ziegler A, Farion R, Decorps M, Remy C (2003) Correlation between the occurrence of 1H-MRS lipid signal, necrosis and lipid droplets during C6 rat glioma development. NMR Biomed 16:199

52. Russell D, Rubinstein LJ (1998) Russel and Rubinstein's Pathology of Tumors of the Nervous System. Arnold, London

53. Levin VA, Leibel SA, Gutin PH (1997) In: De Vita VTj, Hellman S, Rosenberg SA (eds) Cancer Principles and Practice of Oncology, 5th edn. Lippincott-Raven, Philadelphia

54. Cha S (2006) Update on brain tumor imaging: from anatomy to physiology. AJNR Am J Neuroradiol 27:475

55. Martinez-Bisbal MC, Esteve V, Martinez-Granados B, Celda B (2011) Magnetic resonance microscopy contribution to interpret high-resolution magic angle spinning metabolomic data of human tumor tissue. J Biomed Biotechnol 2011:763684. Epub 2010 Sep 5

56. Esteve V, Celda B, Martinez-Bisbal MC (2012) Use of (1)H and (31)P HRMAS to evaluate the relationship between quantitative alterations in metabolite concentrations and tissue features in human brain tumour biopsies. Anal Bioanal Chem

57. Martinez-Bisbal MC, Marti-Bonmati L, Piquer J, Revert A, Ferrer P, Llacer JL, Piotto M, Assemat O, Celda B (2004) 1H and 13C HR-MAS spectroscopy of intact biopsy samples ex vivo and in vivo 1H MRS study of human high grade gliomas. NMR Biomed 17:191

58. Cheng LL, Ma MJ, Becerra L, Ptak T, Tracey I, Lackner A, Gonzalez RG (1997) Quantitative neuropathology by high resolution magic angle spinning proton magnetic resonance spectroscopy. Proc Natl Acad Sci USA 94:6408

59. Cheng LL, Anthony DC, Comite AR, Black PM, Tzika AA, Gonzalez RG (2000) Quantification of microheterogeneity in glioblastoma multiforme with ex vivo high-resolution magic-angle spinning (HRMAS) proton magnetic resonance spectroscopy. Neuro-oncology 2:87

60. Sitter B, Bathen TF, Tessem M, Gribbestad IS (2009) High-resolution magic angle spinning (HR MAS) MR spectroscopy in metabolic characterization of human cancer. Prog Nucl Magn Reson Spectrosc 54:239

61. Lindon JC, Beckonert OP, Holmes E, Nicholson JK (2009) High-resolution magic angle spinning NMR spectroscopy: Application to biomedical studies. Prog Nucl Magn Reson Spectrosc 55:79

Table 1. Sample list including weight and grade classification

Sample	Grade	Weight (mg)
1	GBM (IV)	35.8
2	GBM (IV)	9.8
3	GBM (IV)	21.0
4	GBM (IV)	20.0
5	GBM (IV)	49.0

Figure captions

Fig. 1 Microscopy and spectroscopy results of a heterogenous glioblastoma sample (sample 1). A) Optical image of the sample inside the NMR tube (left) and a 3D NMR image reconstruction (right). B, C) RARE images (50 µm slice thickness) showing internal details and dimensions of this very heterogeneous sample. D) Histological section (H&E staining) with some magnifications that include regions of necrosis, high cellularity and vessels details. E) Several ^{1}H spectra obtained in localized volumes as indicated are presented at right of the image. The signals of the main metabolites are assigned. Differences in the spectra reflect the different metabolic profiles of each region. A mean spectra was obtained for all regions (bottom). F) Image and spectrum from other piece of the same biopsy (sample 2). The spectrum corresponds to the volume indicated in the sagittal (sag) axial (ax) and coronal (cor) images.

Fig. 2 NMR microscopy images and spectra for a homogeneous glioblastoma sample (sample 3). Despite the fact that this sample shows several anatomical features as some big vessels with diverse diameter and tortuosity (A and B), the localized spectra display a remarkable similarity (C). The search for maximum differences in bigger localized volumes around the sample only provided little differences as can be appreciated in the superimposed spectra (D). (A-D) RARE images of 50 µm of thickness, with the zoomed area (A and B) displaying a blood vessel of 330 µm of diameter (A) and a tortuous vessel (B). (D) Three locations for the single voxel and the corresponding spectra overlapped with the assignment for the main resonances (zoom of the 3-4 ppm range at the top left).

Fig. 3 NMR microscopy images and spectra for a necrotic glioblastoma sample (sample 4). A and B) RARE image of a 50 µm thickness slice. C) Distribution of lipids according to the integration of the peak at 5.34 ppm (left). Some localized spectra are shown on the right with an indication of the assignments to the diverse type of hydrogens of a standard aliphatic lipid chain. This piece of tissue is very heterogeneous as can be appreciated in the images A and B. The metabolic profile dominated by the lipids signals indicates a high level of necrosis, nevertheless the profiles are far to be homogenous throughout the whole sample

Fig. 4 Micro-anatomical analysis of the biopsies by NMR microscopy (sample 5). A) Optical image of a histological section (H&E staining) B) Comparative image section by NMR. The distances of some vessels inside the sample area labeled which are similar to the ones on image A. C and D) NMR images of different sections with details on vessel ramification and size. E) Image reconstruction of the whole sample from NMR images. F) 3D model of the vessels distribution inside the sample (the colored spots mark the reference planes).

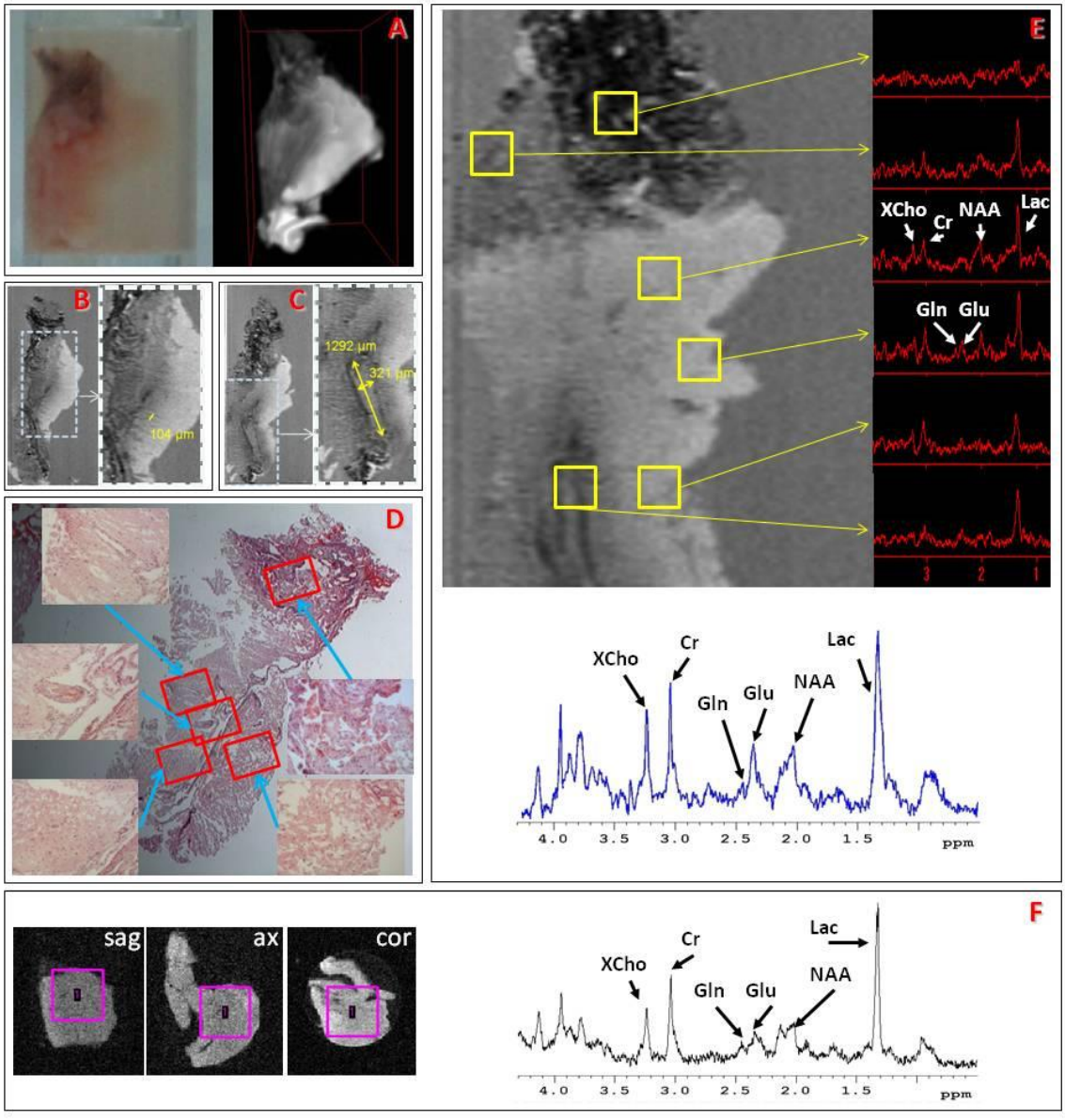

Figure 1

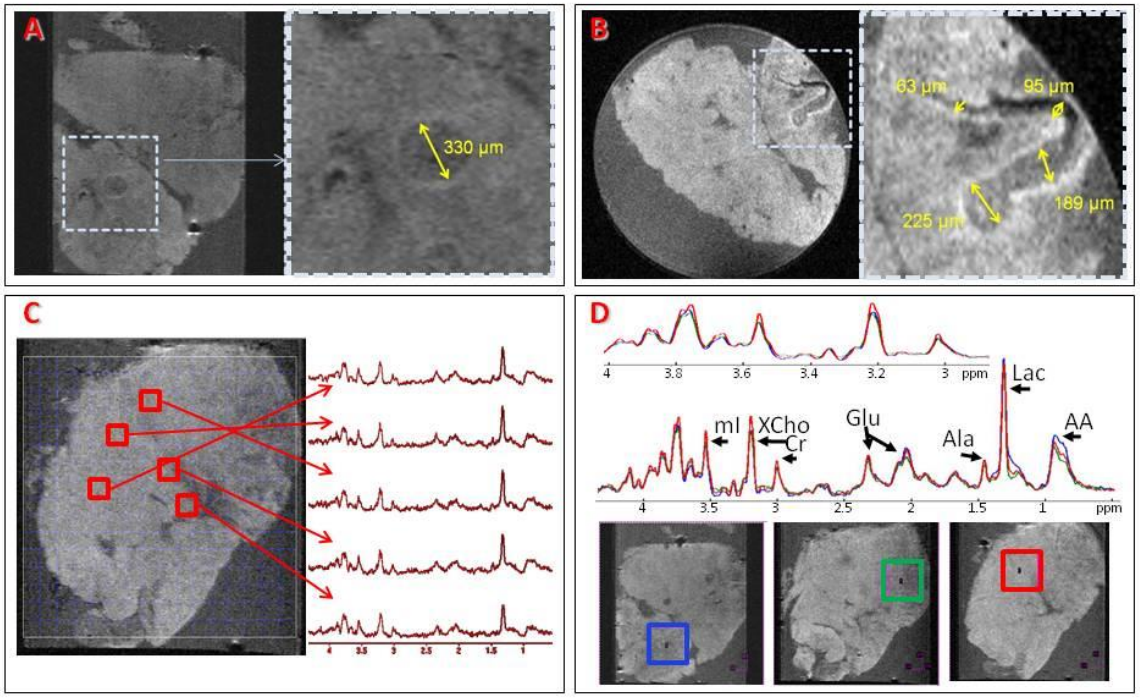

Figure 2

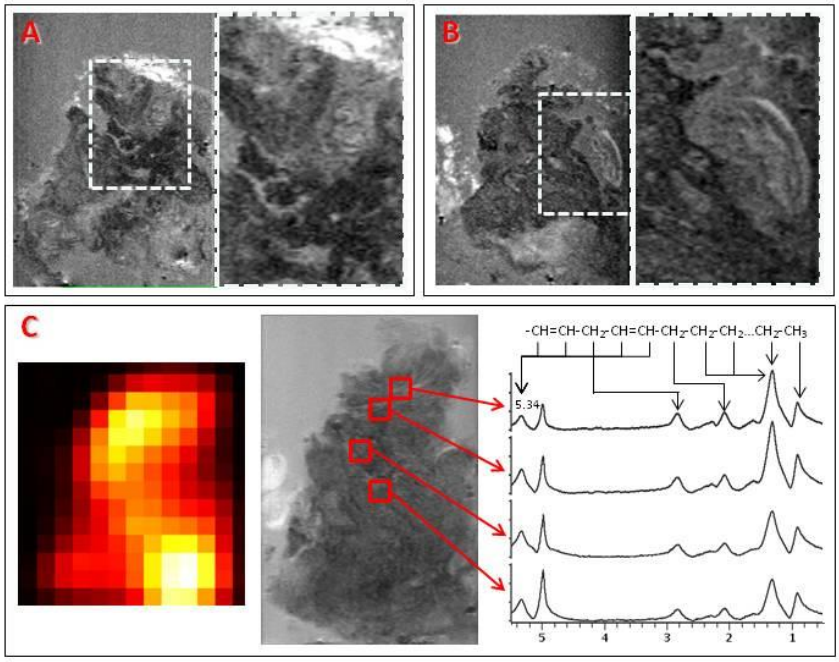

Figure 3

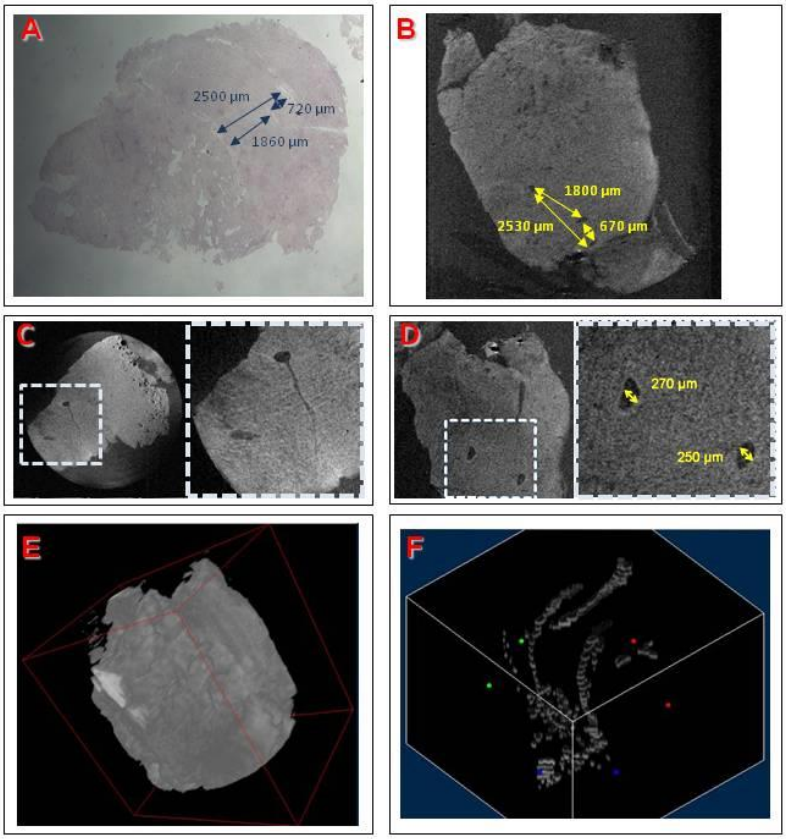
A
2500 µm
720 µm
1860 µm
B
1800 µm
2530 µm
670 µm
C
D
270 µm
250 µm
E
F

Figure 4